Universiteit Leiden
The Netherlands

Theory and kinetic modeling of electrochemical cation-coupled electron transfer reactions

Koper, M.T.M.

ORIGINAL PAPER

Theory and kinetic modeling of electrochemical cation-coupled electron transfer reactions

Marc T. M. Koper[1]

Abstract

A simple Hamiltonian Marcus-type model for cation-coupled electron transfer reactions is introduced, and an expression for the activation energy is derived. The expression is mathematically similar to the classical Frumkin correction. The model explains how cations lower the activation energy for the Volmer reaction in alkaline media and how cations help stabilizing the first intermediate in electrochemical CO_2 reduction. The second part of the paper introduces the cation effect in a more empirical way in an effective rate law and shows how coupling to local pH changes and the corresponding interfacial cation concentration leads to deviations from the standard Butler-Volmer behavior and to non-linear Tafel plots.

Introduction

It is an honor to contribute this paper to the memory of Professor Alexander Milchev. I have many good memories of my stimulating interactions with Alexander, from my PhD, through my postdoc, to my junior and senior scientific career. Alexander was an intellectual giant of electrochemistry, deeply interested in the fundamentals of electron transfer. This paper deals with an old problem in electrode kinetics and electrocatalysis, namely how the interfacial double layer structure influences the rate of electron transfer reactions and how that effect may impact the electrochemical current–potential characteristics.

The structure of the electrolyte near the electrode, and in particular the presence of cations, can indeed have a substantial impact on the rate of electrode reactions. This idea goes back to the seminal work of Frumkin, who modeled this effect by the influence that the local cation concentration has on the potential in the "reaction plane" [1, 2]. In principle, that potential can be calculated from the Gouy-Chapman-Stern theory [3], if one makes suitable assumptions about the location of the reaction plane.

In recent years, there has been growing interest in the role of the electrolyte on the rate and selectivity of electrocatalytic reactions, with special emphasis on the effect of cations [4–6]. It has been shown that especially for reduction reactions such as CO_2 reduction (CO2RR) [7–9] and water reduction to hydrogen [10–12] (hydrogen evolution reaction (HER)), the reaction rate is strongly coupled to the nature and the concentration of electrolyte cations. For the HER on gold electrodes, we established that in a certain range of local cation concentration, cations promote the HER rate [10]. On the other hand, at high cation concentration, the HER rate appears to be adversely affected by the local concentration of cations. These effects have been observed for both gold and platinum electrodes [10, 11] and presumably relate to the cation effects on the HER rate on mercury electrodes observed decades ago [13], studies that served as an initial inspiration for Frumkin to formulate his "cation theory" [2]. A recent short review on cations effects on HER has been published by Ringe [14]. Electrolyte effects on electron-transfer rates have also been highlighted in other areas of inorganic chemistry and electrochemistry [15, 16].

In this short paper, I will first propose a simple Marcus-type theory which introduces an electrostatic interaction between the reactant "Ox" and the cation "cat," which lowers the energy barrier for electron transfer (ET) and the associated bond breaking. I will refer to this as cation-coupled electron transfer (CCET). The model is equivalent to the Frumkin model, but interprets the effect of the cation as a more specific local effect, rather than its effect on the mean-field potential in the reaction plane [1]. Fraggedakis et al. [17], Bazant [18] and Nazmutdinov et al. [19] have recently formulated similar models, motivated by experimental results on electrochemical ion insertion in solid (oxide)

✉ Marc T. M. Koper
  m.koper@chem.leidenuniv.nl

[1] Leiden Institute of Chemistry, Leiden University,
  2300 RA Leiden, The Netherlands

materials and by the effect of ion pairing on the rate of electron transfer and electroplating reactions, respectively. The model presented here applies explicitly to electrocatalysis by building on a Hamiltonian formulation of Savéant's model for bond-breaking electron transfer (BBET) [20, 21]. The model demonstrates how the reactant to be reduced benefits from the (electrostatic) interaction with cations, either by lowering the activation energy for BBET or by stabilizing an intermediate surface-adsorbed ion-pair state. These situations correspond to those envisaged to happen during HER and CO2RR, showing the applicability of this theoretical framework in understanding environmental effects in electrocatalysis. Mathematically, the model provides an extension of the Frumkin correction into the Hamiltonian-based Marcus-type theory of electrochemical electron transfer reactions. In the second part of the paper, I will then introduce a more empirical equation accounting for cation effects on the rate of proton-coupled electron transfer reactions, to illustrate how the current–voltage characteristics of such reactions are expected to exhibit unusual mass transport limitations [10], translating into anomalous Tafel behavior that cannot be considered purely kinetic.

Hamiltonian and ground-state potential energy surface

The reaction modeled here is of the following type:

$$R - X + e^- + \text{cat}^+ \rightarrow R^. + X^- \cdots \text{cat}^+ \tag{1}$$
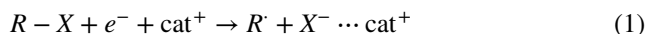
We use here the same notation as in a previous model for bond breaking electron transfer [21], in which $Ox = R–X$ is typically an organic molecule involving a halide bond. However, $R–X$ could be any "Ox" molecule in which an electron is transferred to the lowest unoccupied antibonding molecular orbital, leading to bond weakening and eventually bond breaking upon electron transfer.

The Hamiltonian H of the system consists of four parts:

$$H = H_{\text{elec}} + H_{\text{solv}} + H_{\text{bb}} + H_{\text{int}} \tag{2}$$

The electronic (H_{elec}), solvent (H_{solv}), and bond breaking (H_{bb}) parts of the Hamiltonian are the same as in a previous model suggested by Koper and Voth [21], which was based on Schmickler's original reformulation ($H_{\text{elec}}+H_{\text{solv}}$) of the Anderson-Newns Hamiltonian for describing electrochemical electron transfer (ECET) processes [22]. The H_{int} term is introduced here to account for the (Coulombic) interaction between the reactant and the nearby cation.

Let ε_a be the electronic energy of the abovementioned lowest unoccupied molecular orbital. In second quantized form, the expression for H_{elec} is:

$$H_{\text{elec}} = \varepsilon_a n_a + \sum_k \varepsilon_k n_k + \sum_k \left[V_k c_k^+ c_a + V_k^* c_a^+ c_k \right] \tag{3}$$

where n_a is the occupation number operator of the antibonding orbital, with c_a^+ and c_a the corresponding creation and annihilation operators. The electronic states on the metal are labeled by the quantum number k; $n_k, c_k^+,$ and c_k are the corresponding number, creation, and annihilation operators. The V_k are the corresponding matrix elements. The solvent part is:

$$H_{\text{solv}} = \frac{1}{2} \sum_v \hbar\omega_v \left(p_v^2 + q_v^2 \right) - n_a \sum_v \hbar\, \omega_v g_v q_v \tag{4}$$

where the first term denotes the unperturbed solvent, modeled as a collection of harmonic oscillators; q_v and p_v are the dimensionless coordinates and momenta, ω_v are the frequencies, and v labels the solvent modes. The second term accounts for the interaction between the solvent and the reactant, assumed linear in the charge n_a on the reactant, with g_v as the coupling constant. In this model, the well-known Marcus solvent reorganization energy is given by $\lambda = \sum_v \hbar\omega_v g_v^2/2$ [23]. The third term in Eq. 2 is a switching function which describes the breaking of the bond by the occupation of the antibonding orbital with a metal electron:

$$\begin{aligned} H_{\text{bb}} = &D\left(1 - n_a\right)\left\{ 1 - \exp\left(-a(r - r_0)\right) \right\}^2 \\ &+ Dn_a\exp(-2a\left(r - r_0\right)) \end{aligned} \tag{5}$$

where r is the distance between R and X, r_0 is the equilibrium bond distance, and D the bond dissociation energy. Note that in this model the intact bond ($n_a = 0$) is described by a Morse potential, and the broken bond ($n_a = 1$) by the repulsive part of the Morse potential. The parameter a in Eq. 5 is related to the bond vibration frequency ω_b by $a = \omega_b(\mu/2D)^{1/2}$, with μ the reduced mass of the fragments participating in the bond breaking. Finally, the fourth term in Eq. 2 is the interaction term introduced here, i.e., the interaction between the charge transferred to the reactive system and the charge z on the cation:

$$H_{\text{int}} = -n_a z/\epsilon_s x \tag{6}$$

where x is the distance between the reactant and the cation, and ϵ_s is the relative dielectric constant of the medium. We will consider this interaction mostly at the distance of closest approach x_0, and will refer to $\varphi_{\text{cat}} = z/\epsilon_s x_0$ as the corresponding local cation potential, expressed in units of energy.

Let the generalized solvent reaction coordinate be defined by $q = \sum_v q_v/g_v$. Since all terms coupling to the ET and the reactive system are linear in n_a, the ground-state potential energy surface $E_0(q, r)$ can be calculated in the so-called wide-band approximation, using standard techniques outlined elsewhere [22]:

$$E_0(q,r) = \widetilde{\varepsilon}_a(q,r)\langle n_a(q,r)\rangle + \frac{\Delta}{2\pi}\ln\left(\widetilde{\varepsilon}_a^2(q,r) + \Delta^2\right) + \lambda q^2 + D\{1 - exp(-a(r-r_0))\}^2 \quad (7)$$

with $\langle n_a(q,r)\rangle$ the average occupation of the antibonding orbital, given by

$$\langle n_a(q,r)\rangle = \frac{1}{\pi}\text{arccot}\left(\frac{\widetilde{\varepsilon}_a(q,r)}{\Delta}\right) \quad (8)$$

and

$$\widetilde{\varepsilon}_a(q,r) = \varepsilon_a - 2\lambda q - D\{1 - 2\exp\left(-a(r-r_0)\right)\} - \varphi_{cat} \quad (9)$$

The energy width parameter Δ is a measure for the strength of the electronic coupling between the antibonding orbital and the metal electronic states:

$$\Delta = \pi \sum_k |V_k|^2(\varepsilon - \varepsilon_k) \quad (10)$$

It is well known that Eq. 7 predicts a potential energy surface (PES) with either three stationary states, i.e., two minima and one maximum or saddle point representing reactant, product and transition state, resp., or a single minimum, with the two situations primarily depending on the value of Δ [21, 22]. By the Hellman–Feynman theorem, these stationary points satisfy the following equations:

$$q_s = \langle n_a(q_s,r_s)\rangle,\ 1 - \langle n_a(q_s,r_s)\rangle = \exp(-a(r_s - r_0)) \quad (11)$$

Let us consider the situation with three stationary points first, which occurs when $\Delta \to 0$. For a meaningful PES, we need to define the equilibrium situation, in which we consider the product state R and X^- to be infinitely far apart, i.e., $x \to \infty$. The reactant state is given by $n_R = \langle n_a(q = 0, r = r_0)\rangle = 0$ and the product state by $n_P = \langle n_a(q = 1, r = \infty)\rangle = 1$. They have equal energy if $\varepsilon_a = \lambda$, and hence we can introduce an overpotential η by

defining $\varepsilon_a = \lambda + \eta$. For the transition state, φ_{cat} will have a finite value (that is, r is not infinite), and using Eq. 11, we calculate for n_T:

$$n_T = \frac{1}{\pi}\text{arccot}\left(\frac{\lambda + D + \eta - \varphi_{cat} - 2n_T(\lambda + D)}{\Delta}\right) \quad (12)$$

If η, Δ, and $|\varphi_{cat}| \ll \lambda$, D, a good approximation to Eq. 12 is:

$$n_T = \frac{1}{2} + \frac{\eta - \varphi_{cat}}{2(\lambda + D)} \quad (13)$$

Using Eq. 13, we can calculate the free energy of activation:

$$\Delta G_{act} = E_0^T - E_0^R = \frac{\left(\lambda + D + \eta - \varphi_{cat}\right)^2}{4(\lambda + D)} + \frac{\Delta}{2\pi}\ln\left(\frac{\Delta}{(\lambda + D + \eta - \varphi_{cat})^2 + \Delta^2}\right) \quad (14)$$

At the equilibrium potential, in the limit of $\Delta \to 0$, this simplifies to

$$\Delta G_{act}(\eta = 0) = \frac{\left(\lambda + D - \varphi_{cat}\right)^2}{4(\lambda + D)} = \frac{\lambda + D}{4}\left(1 - \frac{\varphi_{cat}}{\lambda + D}\right)^2 \quad (15)$$

showing that the activation energy is lowered by a factor $\left(1 - \frac{\varphi_{cat}}{\lambda + D}\right)^2$ compared to the non-cation coupled (bond breaking) electron transfer, i.e., the expression originally derived by Savéant [20]. This lowering of the activation energy is of course expected, as the transition state is negatively charged. A schematic drawing of this situation for the example of water reduction reaction is given in Fig. 1A.

Again in the limit of $\Delta \to 0$, the transfer coefficient $\alpha = d\Delta G_{act}/d\eta$ is given by:

$$\alpha = \frac{1}{2} + \frac{\eta - \varphi_{cat}}{2(\lambda + D)} = n_T \quad (16)$$

Fig. 1 **A** Stabilization of the transition state for water dissociation by interaction with nearby cation; **B** Stabilization of the adsorbed $CO_2^{2\delta-}$ intermediate by interaction with nearby cation
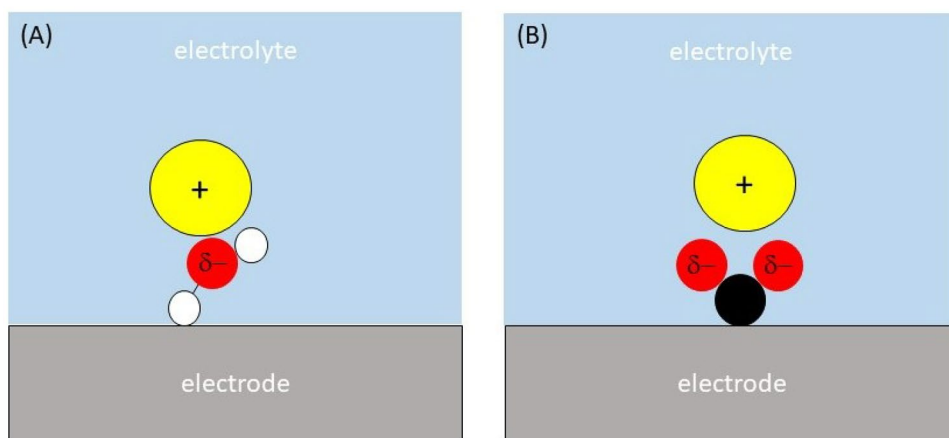
where n_T is the partial charge transferred to the transition state. Interestingly, Eq. 16 predicts that for $\eta = 0$, the transfer coefficient is not ½, but smaller than ½. This is because the interaction with the cation introduces an asymmetry in the PES as the neutral reactant does not interact with the cation, whereas the transition state and the product exit channel do. Unsurprisingly, Eqs. 14 and 16 show that φ_{cat} acts as a local potential to enhance electron transfer, effectively lowering the energy of the transition state in a way that is mathematically equivalent to Frumkin's reaction plane potential [1]. In the PES Eq. 7, there is a state that is more stable than either the reactant or the product state, which is the product X^- state interacting closely (at $x = x_0$) with the cation. In a more complete model, X^- and the cation are expected to separate for entropic reasons.

Next, let us consider the situation in which Δ is not small. A large value of Δ basically means a strong electronic interaction between the metal states and the antibonding orbital of the reactant. It has been previously shown that under these conditions, Eq. 7 predicts a single stationary state which corresponds to an R–X species bonded to the surface by backdonation [21]. The R–X bond does not break, but the species becomes surface adsorbed with a partial charge $\langle n_a(q_s, r_s) \rangle$. The nearby cation then enhances that surface bonding by $\langle n_a(q_s, r_s) \rangle \varphi_{cat}$. This expresses the expected result that a nearby cation enhances the bonding of an adsorbate that acquires a negative charge during the adsorption process. This situation is schematically illustrated in Fig. 1B with the presumed stabilization of adsorbed $CO_2^{\delta-}$ by the interaction with the cation.

In principle, knowing the PES (Eq. 7) also allows one to estimate the actual rate of the reaction, if the dynamics of the reactive system on the PES is known. It is important to point out that we do not consider the electron transfer and the cation dynamics to be concerted, as for instance for some proton-coupled electron transfer reactions (PCET), in which case they are referred to concerted proton-electron transfer (CPET) reactions [24, 25]. This situation is unlikely for cations as cations are typically much heavier particles than protons. Rather, we consider the reaction to be electronically adiabatic, taking place on PES Eq. 7, and the electrons follow the nuclear motion on the PES instantaneously. The PES depends on three reaction coordinates: the collective solvent coordinate q, the distance r between R and X, and the distance x between cation and $(R-)X^-$. The motion on such a multidimensional PES can be described by the approach introduced by Sumi and Marcus [26].

Kinetic modeling of cation-coupled electron transfer reactions

The above model shows that cation-coupled electron transfer should lead to a lowering of the activation energy for electron transfer in a way that is very similar (at least mathematically)

to the Frumkin correction of the Butler-Volmer equation. The model does not specify the exact location of the cation or the cation-intermediate complex; it just specifies their interaction energy φ_{cat}. While Eqs. 14 and 15 predict a lowering of the activation energy and therefore promotion of the reaction rate by cations, I do not consider that the equation itself is very useful for detailed kinetic modeling purposes. For instance, Eq. 15 does not explain why for very high local cation concentration, the rate of HER lowers again [10, 11] (unless one assumes some cation-concentration dependent φ_{cat}, the nature of which then still remains to be elucidated). Moreover, the local cation concentration is not a constant, but in fact depends on the current (density), as it is governed by migration effects. To illustrate the impact of this effect, I use here a more empirical expression for the rate of a cation-coupled (electrocatalytic) electron transfer reaction, specifically the rate-determining Volmer step of HER, which we introduced in ref.[10]:

$$k_V = k_0 \exp\left(\frac{-\alpha F(E - E^0)}{RT}\right) [cat^+]_s^\gamma \tag{17}$$

where the subscript "V" refers to "Volmer", we have used the Butler-Volmer expression for the potential-dependence (i.e., we ignore the quadratic dependence of the activation energy on potential, as predicted by the Marcus model Eq. 14), $[cat^+]_s$ is the local cation concentration (i.e., the interfacial cation concentration at the electrode surface), and γ is an empirical reaction order in (interfacial) cation concentration. A positive value of γ signifies a lowering of the activation barrier by cations:

$$\gamma = \frac{d\ln k_V}{d\ln[cat^+]_s} = \frac{d\Delta G_{act}}{d\varphi_{cat}} \frac{d\varphi_{cat}}{d\ln[cat^+]_s} \tag{18}$$

Equation 17 assumes that the rate of the reaction does not depend on the local pH or OH$^-$ concentration; any pH dependence is apparent and indirect through the dependence on the local cation concentration. The motivation for such a simplification has been discussed in ref. 10 and lies in the fact that it basically reproduces the experimental data in that paper. The complication in predicting the corresponding current–voltage curve arises from the fact that many CCET reactions typically produce OH$^-$. This leads to a higher local concentration of OH$^-$, i.e., a higher local pH. However, just outside the double layer, these newly generated OH$^-$ ions need to be screened electrostatically, that is: local electroneutrality must be satisfied. The system takes care of this by migrating other anions away from the surface and by migrating cations toward the surface. This implies that the local cation concentration actually depends on the local OH$^-$ concentration:

$$[cat^+]_s \approx [cat^+]_b + \beta\left([OH^-]_s - [OH^-]_b\right) \tag{19}$$

where β is a kind of local transference number. Simultaneously, the local OH$^-$ concentration depends on the local mass transport characteristics. At steady state, the generation of OH$^-$ by the CCET reaction and the transport away of OH$^-$ by migration and diffusion must have equal rates. If (convective) diffusion dominates, one can write:

$$k_0 \exp\left(\frac{-\alpha F(E - E^0)}{RT}\right)\left([cat^+]_b + \beta\left([OH^-]_s - [OH^-]_b\right)\right)^\gamma$$
$$= \frac{D}{\delta}\left([OH^-]_s - [OH^-]_b\right) \tag{20}$$

There is no simple solution to this equation, but for argument sake, let us first consider the limiting case of low background concentration of cations. For $[cat^+]_b \approx 0$, one may also assume that $[OH^-]_s \gg [OH^-]_b$, so that it follows that:

$$[cat^+]_s = \beta[OH^-]_s = \left(\frac{k_0 \exp\left(\frac{-\alpha F(E-E^0)}{RT}\right)\delta\beta^\gamma}{D}\right)^{\frac{1}{1-\gamma}} \tag{21}$$

Inserting this expression into the rate of HER gives:

$$j_{HER} \propto k_0 \exp\left(\frac{-\alpha F(E - E^0)}{RT}\right)[OH^-]_s^\gamma$$
$$= k_0 \left(\frac{k_0 \delta\beta^\gamma}{D}\right)^{\frac{\gamma}{1-\gamma}} \exp\left(\frac{-\alpha(1 + \frac{\gamma}{1-\gamma})F(E-E^0)}{RT}\right) \tag{22}$$

Under these (admittedly somewhat extreme) conditions, it follows that the effective transfer coefficient is:

$$\alpha_{eff} = \alpha\left(1 + \frac{\gamma}{1-\gamma}\right) \tag{23}$$

For values of $0 < \gamma < 1$, this shows that the effective transfer coefficient is expected to be larger than the intrinsic transfer coefficient α, and hence the Tafel slope would be smaller than 120 mV/dec (if $\alpha \approx 0.5$). The reason for this is that a higher reaction rate leads to a higher local hydroxide concentration and a correspondingly higher local cation concentration, and hence a higher rate.

In the limit of a high background cation concentration, one can use a Taylor expansion to derive an approximate expression for the reaction rate [10]. However, to illustrate the effect qualitatively, we choose here a particular value for γ which allows to solve Eq. 20, namely $\gamma = \frac{1}{2}$. The expression for the current then becomes:

$$j_{HER} \propto k_0 \exp\left(-\frac{\alpha FE}{RT}\right)\left([cat^+]_b + \beta\left(\frac{\beta + (\beta^2 + 4[cat^+]_b \frac{D^2}{\delta^2 k_0^2} \exp\left(\frac{2\alpha FE}{RT}\right))^{1/2}}{\frac{2D^2}{\delta^2 k_0^2} \exp\left(\frac{2\alpha FE}{RT}\right)}\right)\right)^\gamma \tag{24}$$

This expression shows again that the potential dependence of the reaction rate does not follow a simple Tafel law and that the slope of the Tafel plot does not reflect the intrinsic transfer coefficient α. Also, the experimentally accessible reaction order in the bulk cation concentration $[cat^+]_b$ does not reflect the intrinsic reaction order γ, but something considerably more complicated, due to the interplay with mass transport. Figure 2 shows typical Tafel plots and the corresponding "effective" transfer coefficients (i.e. $\frac{RT}{F}\frac{d\ln j_{HER}}{dE}$) for various values of $D/\delta k_0$, showing how for lower values of the relative mass transport rate (i.e., low $D/\delta k_0$), the deviation from ideal Tafel behavior increases. These non-kinetic effects on the Tafel slope for a reaction for which one intrinsically would not expect mass transport effects were recently also discussed in the experimental context of the oxygen evolution reaction [27].

The primary aim of the above exposition was to illustrate that cation-coupled electron transfer reactions that produce OH$^-$, a reaction type which I believe to be quite ubiquitous in electrocatalysis, are not expected to follow simple Butler-Volmer rate laws. Detailed validation of these models with model systems on model electrodes will be an
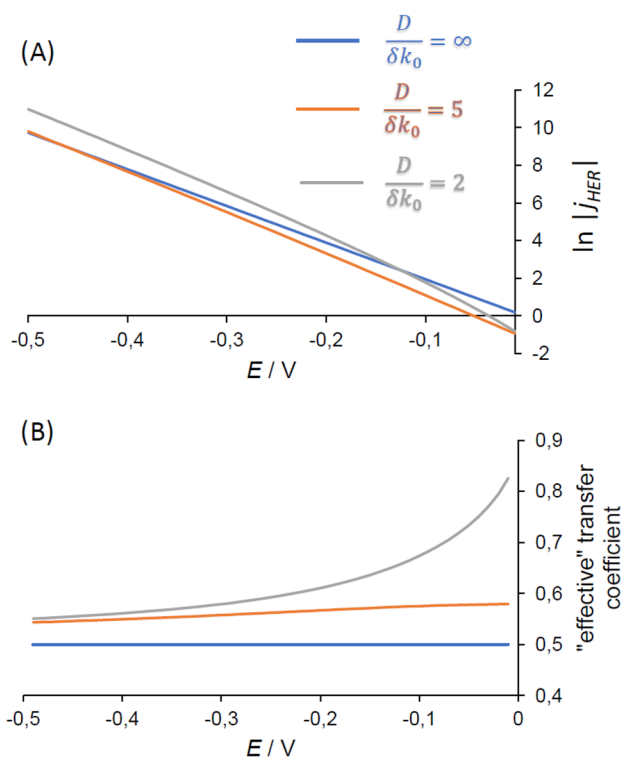

Fig. 2 **A** $\ln |j_{HER}|$ vs. E predicted by Eq. 24, for three different values of $D/\delta k_0$ ($[cat^+]_b = 0.1$ M, $\beta = 0.5$, $\gamma = 0.5$, $\alpha = 0.5$). **B** Corresponding "effective" transfer coefficient extracted from curves in **A**

important topic of future research. Note however that the unexpected mass transport dependence predicted by Eq. 24 (with the reaction current going down for a thinner diffusion layer or higher disk rotation rate, due to the enhanced removal of hydroxide from the interfacial region) has been semi-quantitatively confirmed experimentally for the HER on gold polycrystalline electrodes in alkaline media [10].

Conclusion

In this paper, I have considered a Marcus-type model for cation-coupled electron transfer (CCET) reactions, showing how the interaction with a cation may stabilize a negatively charged transition state or negatively charged surface-adsorbed intermediate. An expression was derived for the activation energy which is similar to the Savéant-Marcus expression for bond-breaking electron-transfer reaction, but including a term which is mathematically equivalent to the Frumkin correction, effectively lowering the activation energy. A simpler more empirically inspired expression for the reaction rate shows how the overall rate of CCET is strongly coupled to the mass transport of the hydroxide ions that the CCET reaction typically produces, as the local hydroxide concentration influences the local cation concentration. The result is a complicated rate expression that does not follow simple Tafel or Butler-Volmer laws and that displays an unusual mass transport dependence. This unusual mass transport dependence has indeed been observed experimentally during hydrogen evolution on a gold electrode in alkaline media [10], in good agreement with the predictions of the model, but other more detailed predictions of the model remain to be validated experimentally.

References

1. Frumkin AN (1933) Z Phys Chem 164:121
2. Frumkin AN (1959) Trans Faraday Soc 55:156
3. Bard AJ, Faulkner LR, White HS (2022) Electrochemical methods: fundamentals and applications, 3rd edn. Wiley
4. Strmcnik D, Kodama K, van der Vliet D, Greeley J, Stamenkovic V, Markovic NM (2009) Nat Chem 1:466
5. Waegele M, Gunathunge CM, Li J, Li X (2019) J Chem Phys 151:160902
6. Marcandalli G, Monteiro MCO, Goyal A, Koper MTM (2022) Acc Chem Res 55:1900
7. Resasco J, Chen LD, Clark E, Tsai C, Hahn C, Jaramillo TF, Chan K, Bell AT (2017) J Am Chem Soc 139:11277
8. Monteiro MCO, Dattila F, Hagedoorn B, García-Mueles R, López N, Koper MTM (2021) Nat Catal 4:654
9. Qin X, Vegge T, Hansen HA (2023) J Am Chem Soc 145:1897
10. Goyal A, Koper MTM (2021) Angew Chem Int Ed 60:13452
11. Monteiro MCO, Goyal A, Koper MTM (2021) ACS Catal 11:14328
12. Bender JT, Petersen AS, Ostergaard FC, Wood MA, Heffernan SNJ, Milliron DJ, Rossmeisl J, Resasco J (2023) ACS Energy Lett 8:657
13. Herasymenko P, Slendyk I (1930) Z Phys Chem A 149:230
14. Ringe S (2023) Curr Opin Electrochem 39:101268
15. Bruhn H, Nigam S, Holzwarth JF (1982) Faraday Disc Chem Soc 74:129
16. Fletcher S, Van Dijk NJ (2016) J Phys Chem C 120:26225
17. Fraggedakis D, McEldrew M, Smith RB, Krishnan Y, Zhang Y, Bai P, Chueh WC, Shao-Horn Y, Bazant MZ (2021) Electrochim Acta 367:137432
18. Bazant MZ (2023) Faraday Disc, in press. https://doi.org/10.1039/D3FD00108C
19. Nazmutdinov R, Quaino P, Colombo E, Santos E, Schmickler W (2020) Phys Chem Chem Phys 22:13923
20. Savéant JM (1987) J Am Chem Soc 109:6788
21. Koper MTM, Voth GA (1998) Chem Phys Lett 282:9840
22. Schmickler W (1986) J Electroanal Chem 204:31
23. Marcus RA (1965) J Chem Phys 43:679
24. Hammes-Schiffer S, Stuchebrukhov AA (2010) Chem Rev 110:6939
25. Koper MTM (2013) Chem Sci 4:2710
26. Sumi H, Marcus RA (1986) J Chem Phys 84:4894
27. Van der Heijden O, Park S, Eggebeen JJ, Koper MT (2023) Angew Chem Int Ed 62:e202216477